

## Supporting Information

### Optimised room temperature, water-based synthesis of CPO-27-M metal-organic frameworks with high Space-Time Yields

L. Garzón-Tovar,<sup>a</sup> A. Carné-Sánchez,<sup>a</sup> C. Carbonell,<sup>a</sup> I. Imaz<sup>a\*</sup> and D. Maspoch<sup>ab\*</sup>

<sup>a</sup> ICN2 (ICN-CSIC), Institut Català de Nanociència i Nanotecnologia, Esfera UAB 08193 Bellaterra, Spain. E-mail: inhar.imaz@icn.cat; [daniel.maspoch@icn.cat](mailto:daniel.maspoch@icn.cat).

<sup>b</sup> Institució Catalana de Recerca i Estudis Avançats (ICREA), 08100 Barcelona, Spain

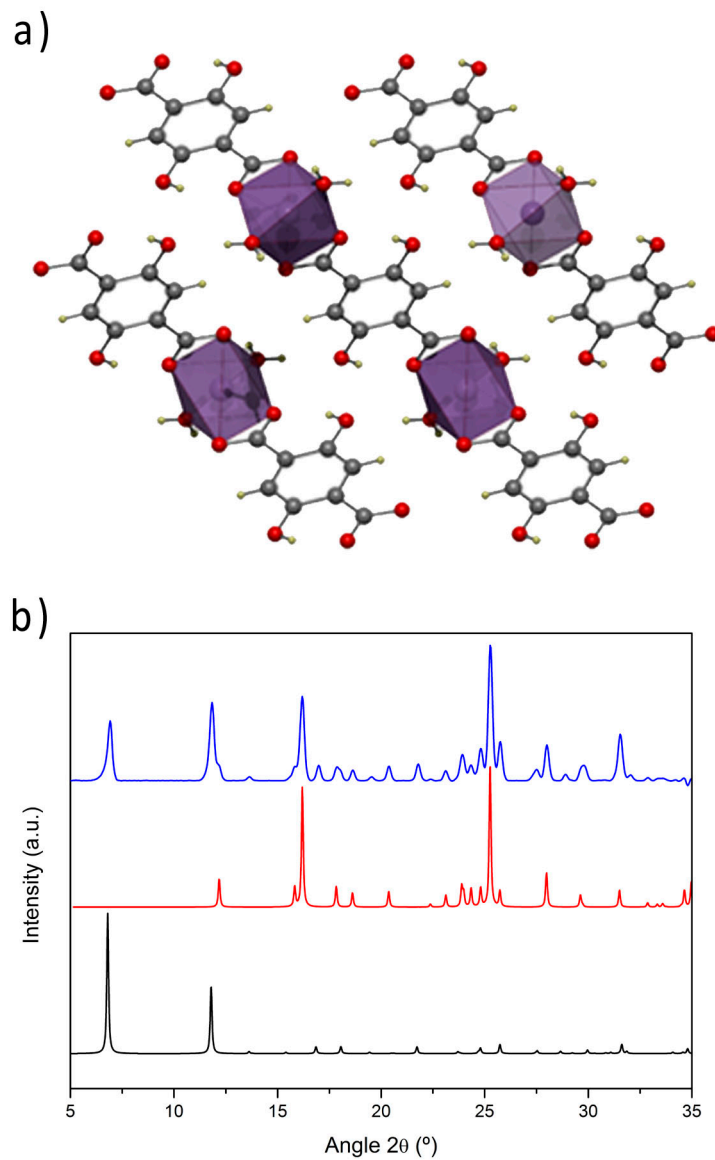


**FIGURE S1:** a) Representation of the structure of  $[\text{Zn}(\text{H}_2\text{O})_2(\text{dhtp})]_n$  coordination polymer, showing the protonated hydroxyl group. b) Comparison of the powder collected after 24 hours of reaction with two equivalents of NaOH (blue), with the simulated powder pattern for CPO-27-Zn (black) and for  $[\text{Zn}(\text{H}_2\text{O})_2(\text{dhtp})]_n$  crystal structure (red).

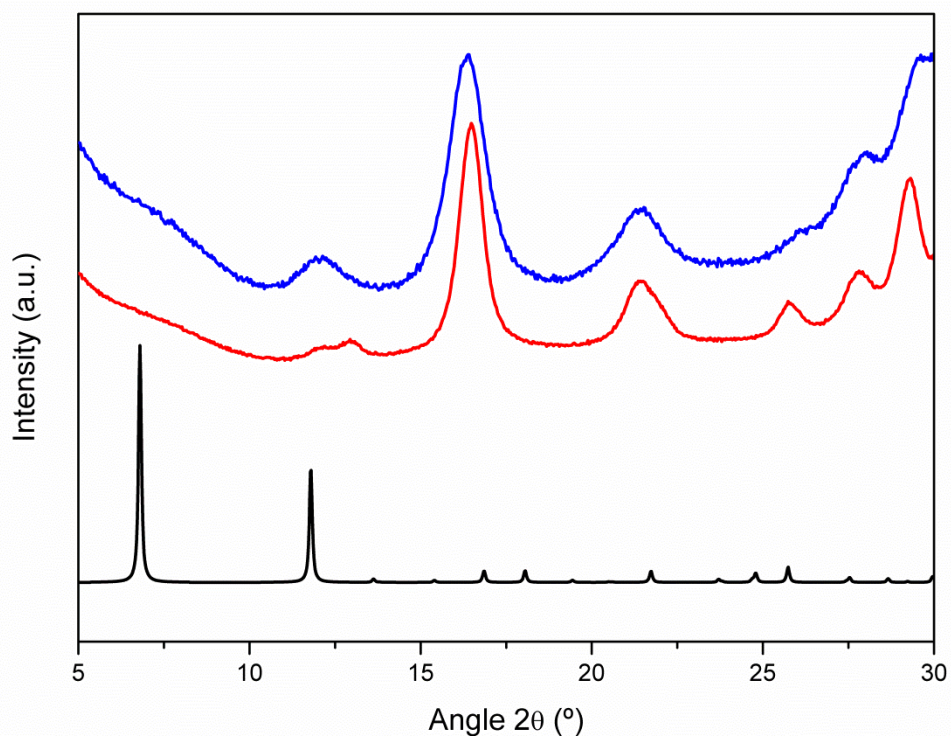


**FIGURE S2:** XRPD diffractograms of the powders collected after the reaction of copper acetate and dhtp using two equivalents (Red) or four equivalents (Blue) of NaOH, as compared to the simulated powder pattern for CPO-27-M (black). The comparison reveals the formation of a new, unknown crystalline phase.

**Table S1:**  $S_{\text{BET}}$  values and yields obtained for CPO-27-Ni and CPO-27-Mg during the optimisation of the reagent concentrations (reaction time = 24 h).

CPO-27-M	$C_1$ ( $\text{mol L}^{-1}$ )	Yield (%)	$S_{\text{BET}}$ ( $\text{m}^2 \text{g}^{-1}$ )
Ni	0.364	99	650
	0.273	98	247
	0.182	94	435
	0.137	92	427
	0.091	75	480
	0.069	76	1351
Mg	0.364	99	1020
	0.273	96	1337

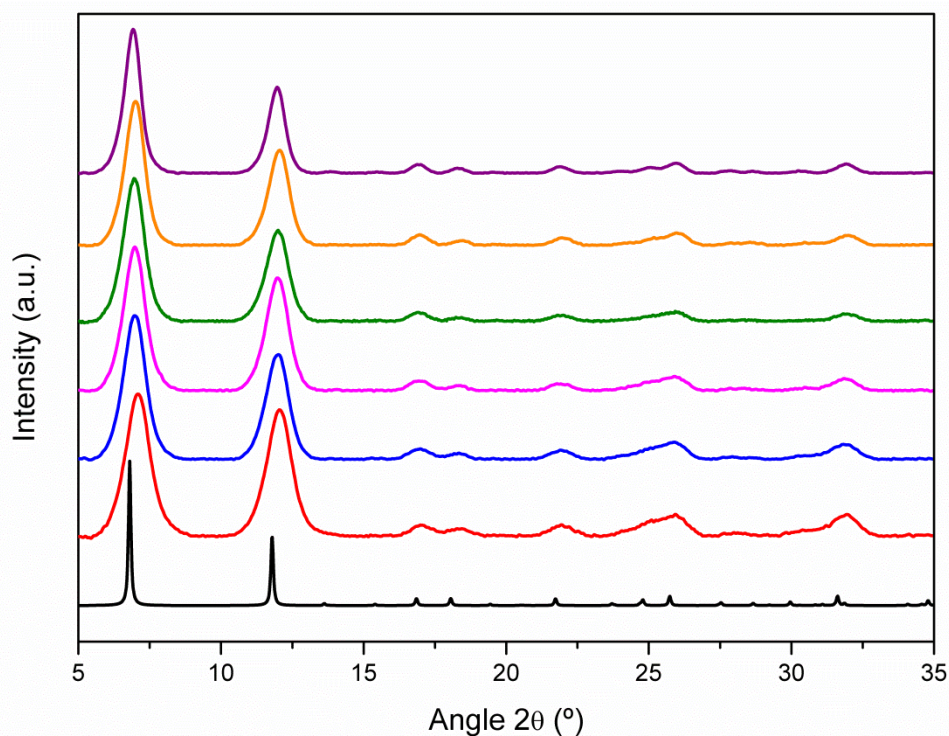


**FIGURE S3:** XRPD diffractograms of the CPO-27-Ni powders collected after their synthesis (using four equivalents of NaOH) at different concentrations (Red:  $C_1 = 0.364 \text{ mol L}^{-1}$ , Blue:  $C_1 = 0.273 \text{ mol L}^{-1}$ , Pink:  $C_1 = 0.182 \text{ mol L}^{-1}$ , Green:  $C_1 = 0.137 \text{ mol L}^{-1}$ , Orange:  $C_1 = 0.091 \text{ mol L}^{-1}$ , Purple:  $C_1 = 0.069 \text{ mol L}^{-1}$ ), as compared to the simulated powder pattern for CPO-27-M.

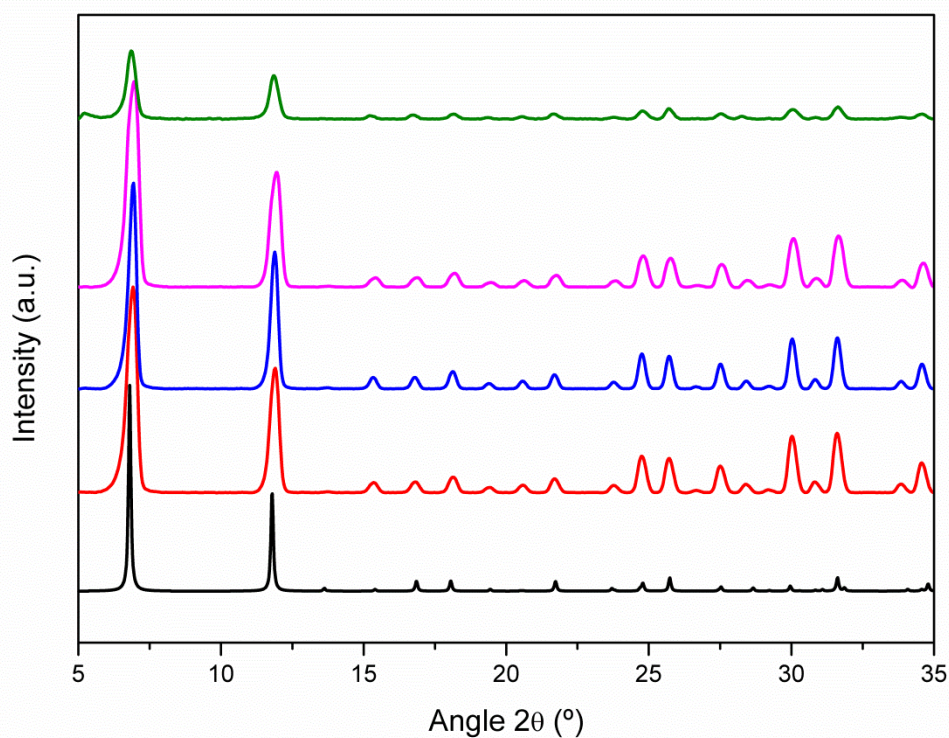


**FIGURE S4:** XRPD diffractograms of the CPO-27-Mg powders collected their synthesis (using four equivalents of NaOH) at different concentrations (Red:  $C_1 = 0.364 \text{ mol L}^{-1}$ , Blue:  $C_1 = 0.273 \text{ mol L}^{-1}$ , Pink:  $C_1 = 0.182 \text{ mol L}^{-1}$ , Green:  $C_1 = 0.091 \text{ mol L}^{-1}$ ), as compared to the simulated powder pattern for CPO-27-M.

**Table S2:**  $S_{\text{BET}}$  values and yields obtained for different CPO-27-Zn, CPO-27-Ni, CPO-27-Mg and CPO-27-Co MOFs synthesised during the optimisation of the reaction time.

CPO-27-M	$C_1$ (mol L <sup>-1</sup> )	Time (h)	Yield (%)	$S_{\text{BET}}$ (m <sup>2</sup> g <sup>-1</sup> )	Pore volume (cm <sup>3</sup> /g) <sup>a</sup>
Zn	0.364	24	98	900	0.34
		12	97	996	0.37
		1	98	1071	0.40
		0.17	98	1279	0.47
		0.08	92	1154	0.44
Ni	0.069	24	76	1351	0.53
		12	78	1304	0.51
		10	84	1029	0.41
		8	86	1043	0.42
		6	92	1220	0.48
Mg	0.273	24	96	1337	0.51
		12	92	1454	0.56
		6	90	1557	0.58
		4	81	1376	0.52
Co	0.364	24	90	1308	0.51
		12	97	1240	0.48
		2	93	1102	0.44
		1	90	962	0.39

<sup>a</sup> Pore volume was calculated at  $P/P_0 = 0.15$  ( $N_2$ , 77 K) using the Quantachrome ASiQWin software.

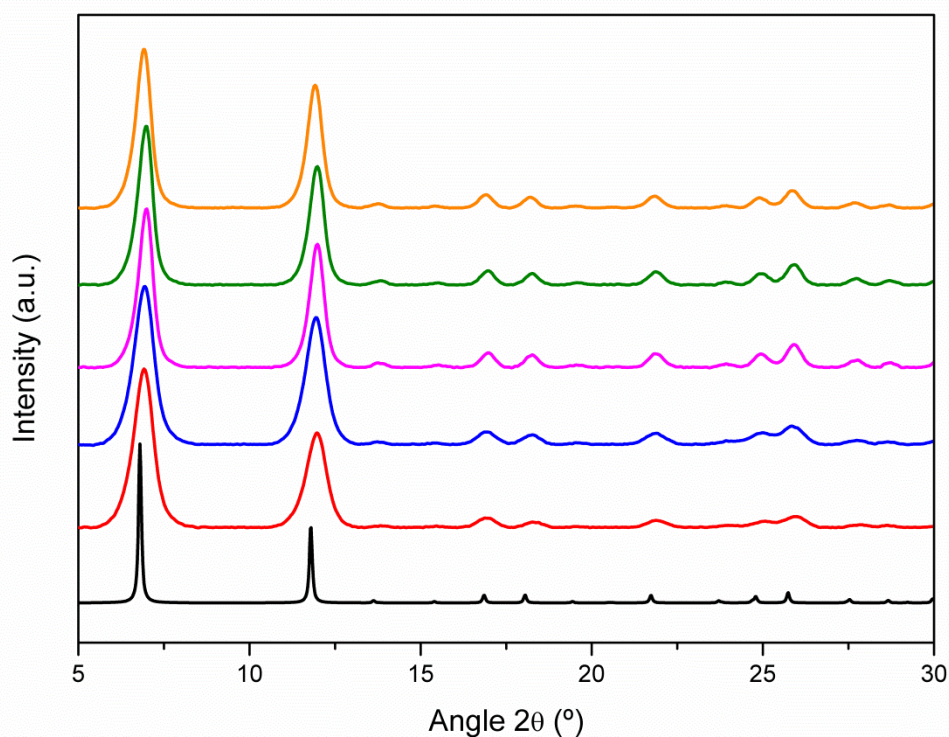


**FIGURE S5:** XRPD diffractograms of the collected CPO-27-Ni powders synthesised using four equivalents of NaOH, at different reaction times (Red: 24 h, Blue: 12 h, Pink: 10 h, Green: 8 h, Orange: 6 h), as compared to the simulated powder pattern for CPO-27-M (black).

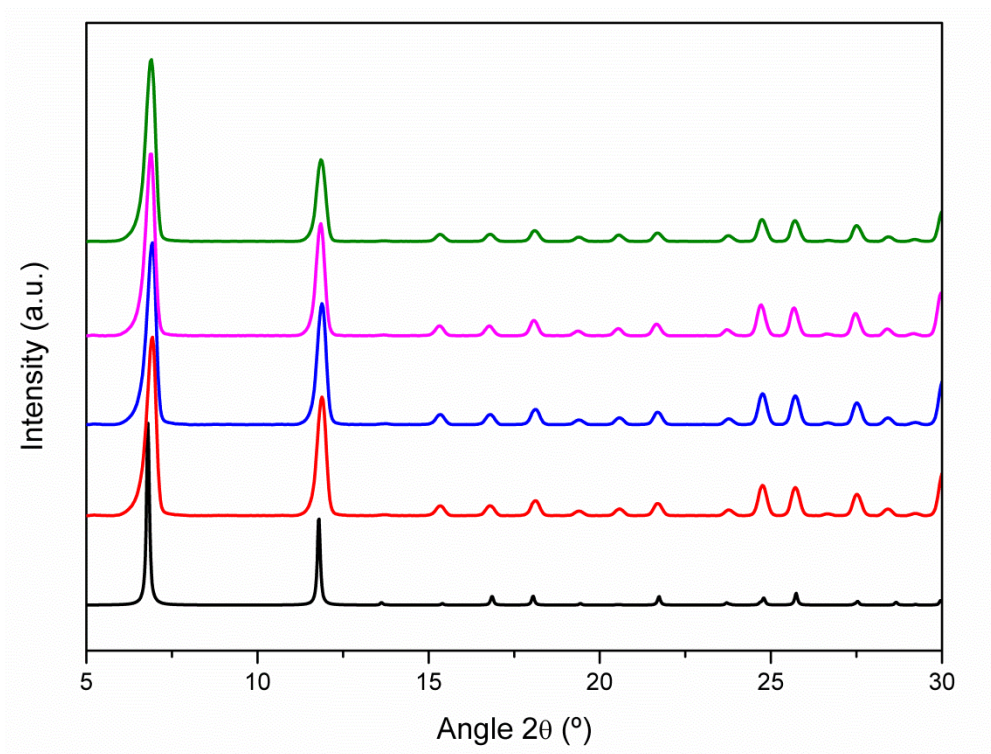


**FIGURE S6:** XRPD diffractograms of the collected CPO-27-Mg powders synthesised using four equivalents of NaOH , at different reaction times (Red: 24 h, Blue: 12 h, Pink: 6 h, Green: 4 h), as compared to the simulated powder pattern for CPO-27-M (black).

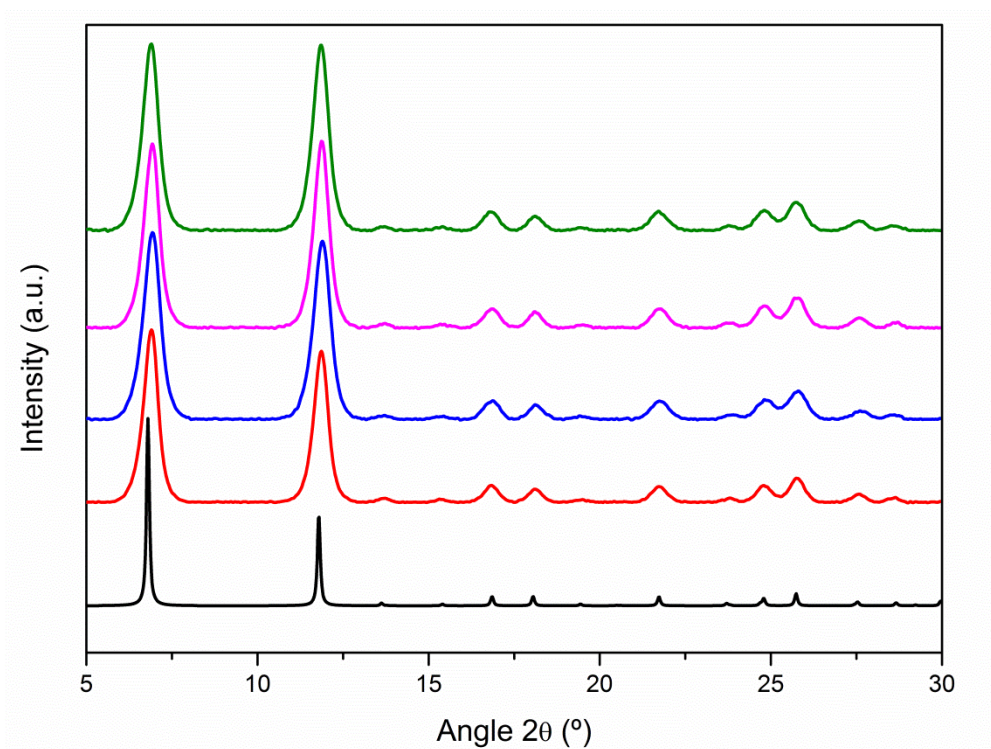


**FIGURE S7:** XRPD diffractograms of the collected CPO-27-Co powders synthesised using four equivalents of NaOH at different reaction times (Red: 24 h, Blue: 12 h, Pink: 2 h, Green: 1 h), as compared to the simulated powder pattern for CPO-27-M (black).

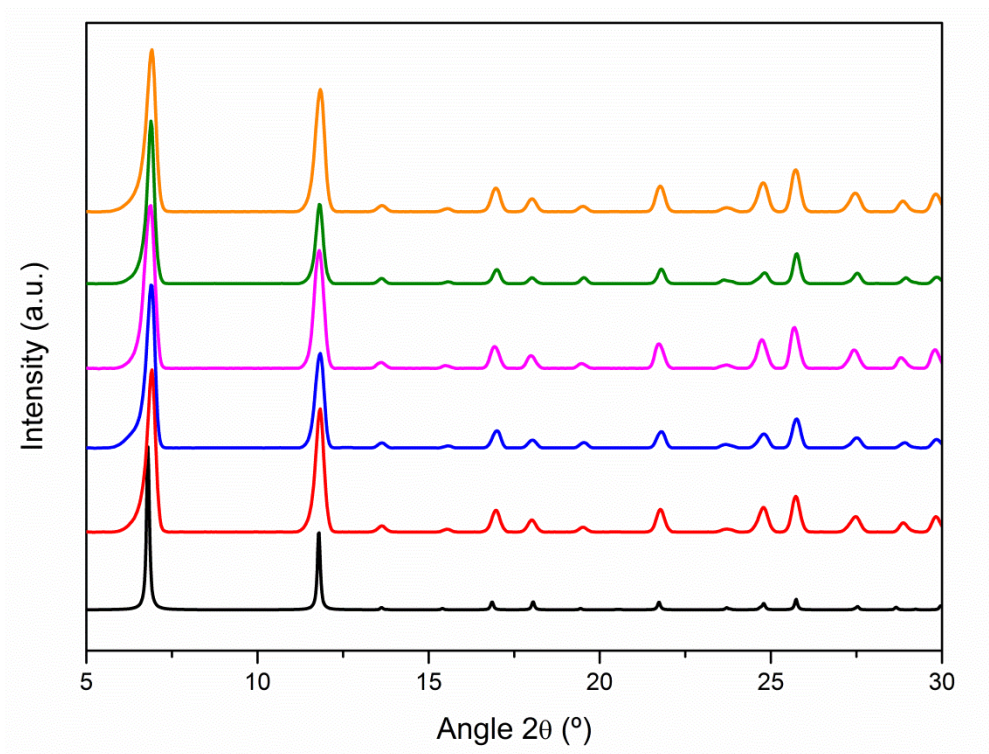


**FIGURE S8:** XRPD diffractograms of the collected CPO-27-Zn powders synthesised using four equivalents of NaOH at different reaction times (Red: 24 h, Blue: 12 h, Pink: 1 h, Green: 10 min, Orange: 5 min), as compared to the simulated powder pattern for CPO-27-M (black).

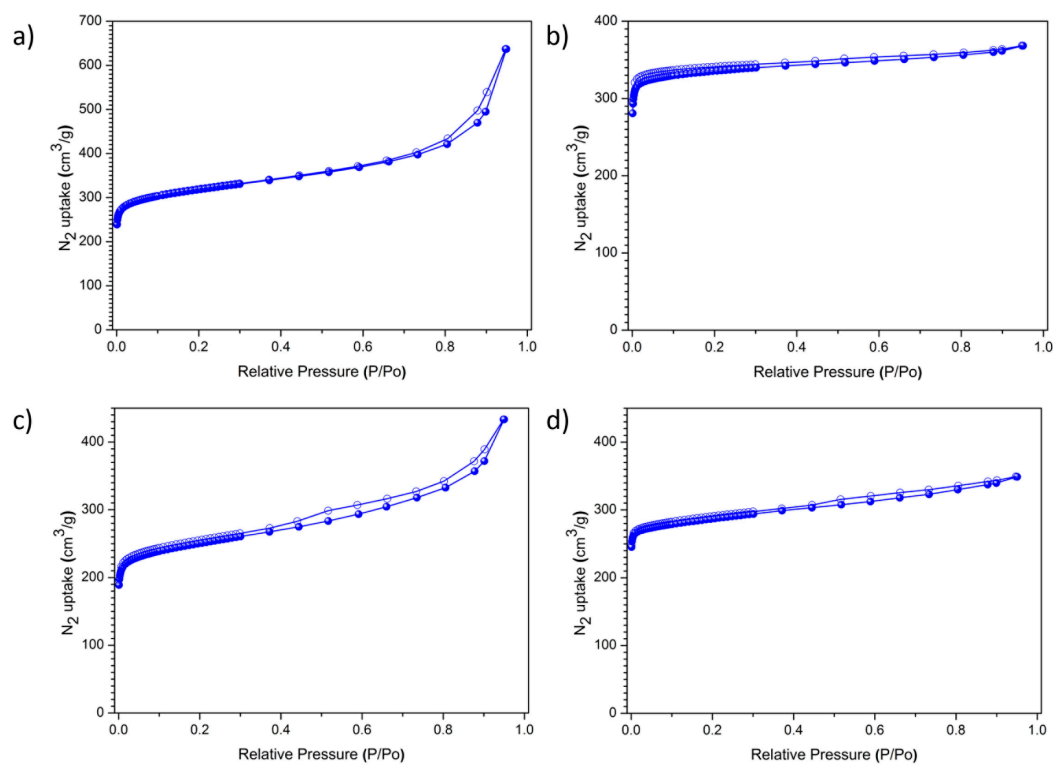


**FIGURE S9:**  $N_2$  adsorption isotherms of the synthesized a) CPO-27-Ni, b) CPO-27-Mg, c) CPO-27-Co and d) CPO-27-Zn showing the corresponding maximum STY values.

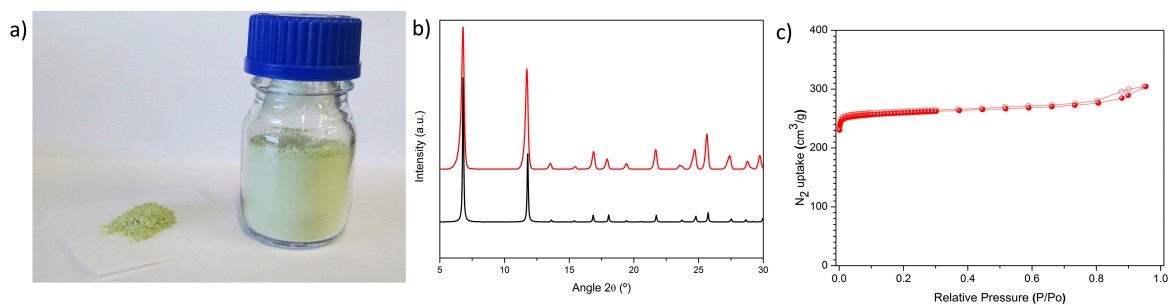


**FIGURE S10:** a) Photograph of CPO-27-Zn powder synthesised at the gram scale. b) XRPD diffractogram of this powder compared to the simulated powder pattern for CPO-27-M (black). c) N<sub>2</sub> adsorption isotherm of the collected powder.

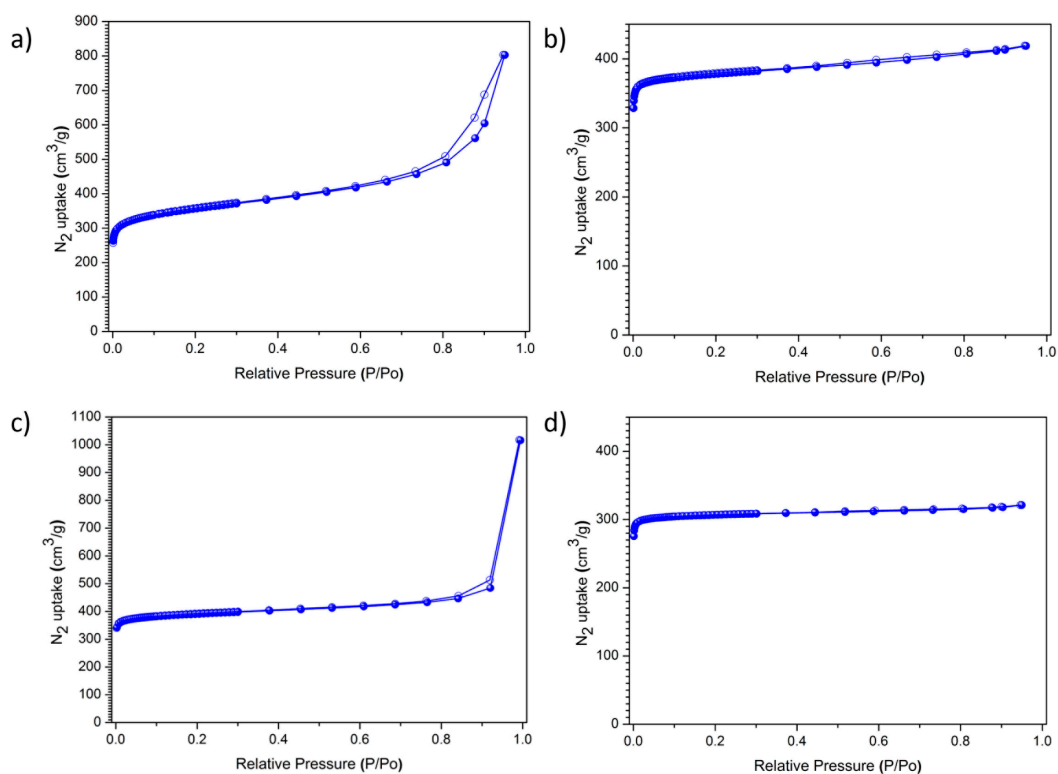


**FIGURE S11:** N<sub>2</sub> adsorption isotherms of the synthesized a) CPO-27-Ni, b) CPO-27-Mg, c) CPO-27-Co and d) CPO-27-Zn showing the corresponding maximum  $S_{\text{BET}}$  values.

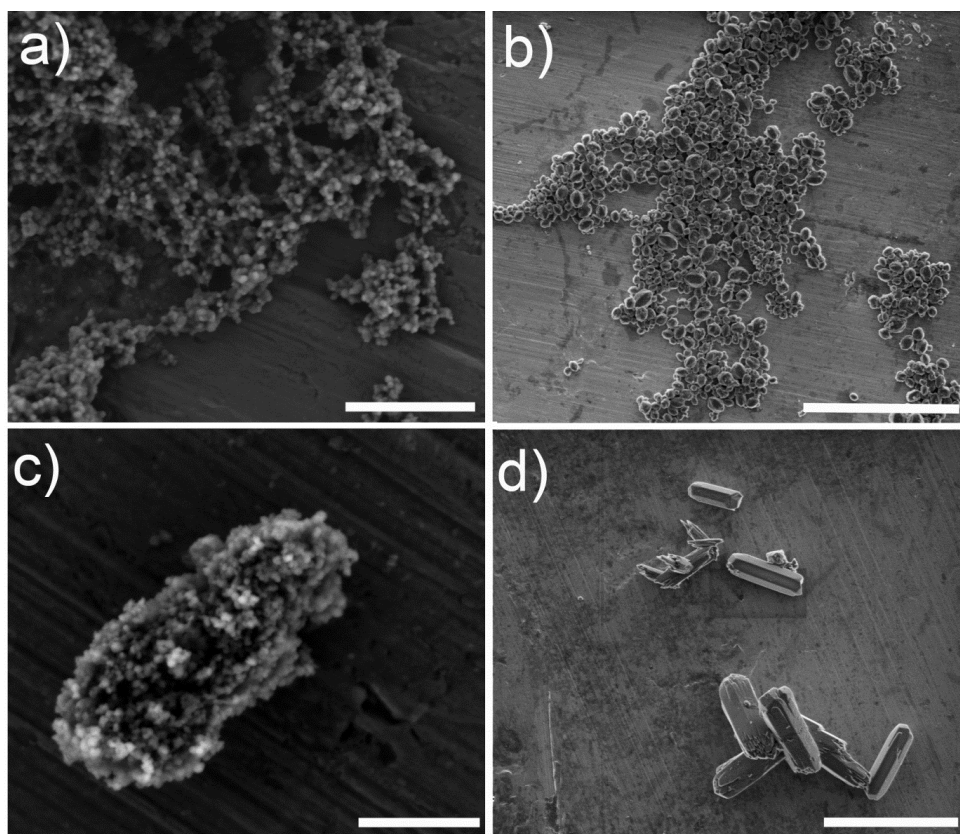


**Figure S12:** FESEM images of the synthesised a) CPO-27-Ni, b) CPO-27-Mg, c) CPO-27-Co and d) CPO-27-Zn, showing the corresponding maximum SBET values. The dimensions of these crystals are  $29 \pm 5$  nm for CPO-27-Ni,  $0.8 \pm 0.1 \mu\text{m} \times 0.6 \pm 0.1 \mu\text{m}$  for CPO-27-Mg,  $50 \pm 5$  nm for CPO-27-Co, and  $5.1 \pm 0.9 \mu\text{m} \times 1.6 \pm 0.4 \mu\text{m}$  for CPO-27-Zn. Scale bars are a)  $1 \mu\text{m}$ , b)  $10 \mu\text{m}$ , c)  $500$  nm, and d)  $10 \mu\text{m}$ .